Proceedings of the 21st ICSMGE, Vienna, Austria, 14 – 19 June 2026. Pistrol, Adam & Schweiger (eds.)
Published by: ÖGG, Austrian Society for Geomechanics, Salzburg, Austria, ISBN 978-3-9503898-4-5
https://doi.org/10.53243/ICSMGE2026-2256

Investigation of Performances of Foundations on Improved Soil Conditions During Seismic Soil Liquefaction

Pelin Özener

Professor, Department of Civil Engineering, Yildiz Technical University, Türkiye, tohumcu@yildiz.edu.tr

Ömer Işkın
MSc. Geotechnical Engineer, Yildiz Technical University, Türkiye, omer.iskin@std.yildiz.edu.tr

ABSTRACT: After the Kahramanmaraş-Pazarcık (M_w=7.8) and Elbistan (M_w=7.5) earthquakes, site studies were conducted in earthquake-affected districts to examine the effects of site conditions on the performance of superstructures. Onsite observations in liquefied regions revealed that some buildings had sustained structural damage, leading to excessive rotation, settlement, or collapse. In contrast, other buildings in the same areas showed no structural damage and performed well. In this study, a layered liquefiable soil profile inspired by the geological conditions of the İskenderun district, Hatay province, Türkiye, was modeled in Plaxis 2D using the PM4Sand and PM4Silt constitutive models. Based on configurations inspired by a building located in Hatay, the seismic performance of buildings with different foundation systems was evaluated. These systems include shallow raft foundations with one and two basement floors; and unreinforced pile foundations without a basement, with one basement, and with two basements. For each configuration, the excess pore pressure ratio, shear strains, horizontal and vertical displacements with depth, and total and differential settlements beneath the buildings were calculated. Angular rotations of the superstructures were also determined. The results were then compared against international engineering standards and guidelines to assess structural performance. Findings indicate that increasing foundation depth consistently improves structural performance across all systems. The best performance was observed in the structure with two basement floors and an unreinforced pile foundation, while the lowest performance was associated with the single-basement raft foundation. These results highlight the critical influence of foundation types on the seismic behavior of structures.

KEYWORDS: Liquefaction, Pm4Sand, Pm4Silt, different foundation types, building performance.

1 INTRODUCTION

Soil liquefaction has long been recognized as a critical topic in geotechnical engineering. Research efforts aimed at understanding the mechanism of this phenomenon and mitigating its effects began with Casagrande's introduction of the concept of critical void ratio in 1936, and gained momentum with the incorporation of the term "liquefaction" into the literature by Terzaghi and Peck in 1948 (Casagrande, 1936; Terzaghi and Peck, 1948). Subsequently, researchers such as Mogami and Kubo (1953) extensively investigated the behavior of liquefaction under cyclic loading conditions (Mogami and Kubo, 1953).

Today, advanced constitutive models such as PM4Sand and PM4Silt have significantly advanced liquefaction assessments by providing more realistic simulation results. While the PM4Sand model is employed to simulate the seismic behavior of sandy soils, the PM4Silt model is preferred for analyzing the behavior of silty and clayey soils with low plasticity. These models, when integrated into finite element-based analysis software such as Plaxis 2D, enable more reliable estimates of lateral and vertical displacements, shear strains, and excess pore water pressures during seismic events (Dafalias and Manzari, 2004).

The PM4 constitutive models (PM4Sand / PM4Silt) provide an advanced constitutive description for simulating cyclic behavior and pore-pressure generation in sandy and fine-grained soils. On the other hand, it has several limitations that should be acknowledged. Firstly, PM4 models are calibrated primarily for uncemented, cohesionless, or weakly cohesive soils and may not accurately capture the behavior of heavily cemented, fissured, or highly organic deposits. Secondly, the model's predictions of pore-pressure accumulation and post-liquefaction stiffness and strength are sensitive to input calibration (e.g., CRR curves, convective parameters) and to the quality of the laboratory data used. Therefore, inadequate calibration can produce unrealistic results. Thirdly, rate-dependent effects, temperature, and chemical alterations are outside the model's formulation. Finally, numerical implementation (mesh density, boundary conditions, and coupling scheme) can affect predicted responses and needs to be considered when interpreting results. Overall, the present numerical results should be interpreted with these limitations in mind and validated against experimental and observational evidence.

Various soil improvement techniques have been developed to prevent structural damage caused by liquefaction (Bray and Dashti, 2014). Among these methods, diaphragm walls, jet grout columns, and unreinforced piles are commonly used to strengthen foundation systems. In addition, the presence of a basement in the building plays a decisive role in the structural performance under liquefaction. Together with structural loads, such soil improvement applications can be modeled using numerical tools such as Plaxis 2D, enabling a comprehensive evaluation of structural performance. These evaluations are expressed through parameters such as total settlements, differential settlements, and tilting behavior of the structure (Bird et al., 2005).

The scope of this study is to investigate the seismic performance of buildings with different foundation systems by conducting numerical analyses using the PM4Sand and PM4Silt constitutive models. The analyses are inspired by the observed behavior of a building located on liquefiable soil conditions in the Çay District of İskenderun, Hatay Province, during the February 6, 2023, Kahramanmaraş Earthquakes. A representative soil profile was developed based on the local soil conditions in İskenderun, and the seismic performance of buildings with varying foundation systems was analyzed. The study aims to evaluate the effects of different foundation configurations on building performance under seismic soil liquefaction conditions.

2 NUMERICAL ANALYSES

In this study, a two-dimensional soil model was developed based on the ISK-275 borehole log, consisting of sand with a relative density of 35% and silty clay with a plasticity index of 20%. Dynamic analyses were performed using the PM4Sand and PM4Silt constitutive models available in Plaxis 2D. The buildings analyzed were designed as seven-story structures with a foundation width of 25 meters.

The structures modeled include: (i) buildings with a raft foundation system incorporating one and two basement floors, and (ii) buildings with unreinforced pile foundations designed as basement-free (with a foundation depth of 1 meter), with one basement floor (3 meters deep), and with two basement floors (6 meters deep).

As a result of seismic soil liquefaction, the variations in settlements beneath the center of the building foundations, lateral displacements, shear strains, and excess pore water pressure ratios with depth were examined. To evaluate the structural performance of the buildings, the maximum settlement, differential settlement, and angular distortion values were calculated. These values were then assessed in accordance with internationally recognized civil engineering standards and codes of practice to determine whether they remained within acceptable limits.

2.1 *Earthquake Record*

The earthquake record used in this study corresponds to the first mainshock ($M_w = 7.8$) of the February 6, 2023, Kahramanmaraş Earthquakes. It was obtained from the TK-3116 station, the closest recording station to the study area in the İskenderun district, which did not experience any interruptions during the earthquake. The raw acceleration-time record retrieved from the AFAD (Disaster and Emergency Management Authority) Türkiye Strong Motion Database and Analysis System is presented in Figure 1.

It was observed that the portion of the 125-second acceleration-time record with the highest amplitudes occurred between 58 and 90 seconds. Accordingly, the 32-second segment of strong motion within this interval was selected for the numerical analyses. The selected ground motion was corrected for baseline using DeepSoil v7, and displacement correction was applied during analyses in Plaxis 2D. The baseline-corrected earthquake record is shown in Figure 1, while the key characteristics of the strong ground motion are presented in Table 1.

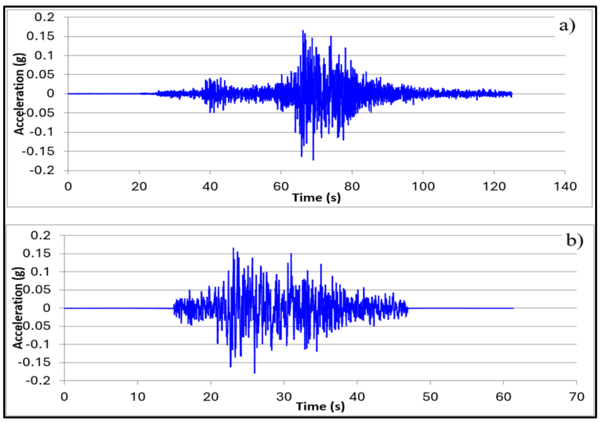

Figure 1. a) Raw acceleration–time record obtained from the TK3116 station, b) Acceleration–time record from the İskenderun station used in the analyses

Table 1. Seismic parameters of the Kahramanmaraş earthquake used in the numerical analyses.

Earthquake	Kahramanmaraş Earthquake Sequence
Station Code	TK-3116
M_w	7.8
PGA (g)	0.17
f_{eq} (Hz)	1.59
I_a (m/s)	0.77

2.2 *Numerical Model*

Before the February 6, 2023, Kahramanmaraş Earthquakes, a geotechnical site investigation was conducted in the İskenderun district of Hatay Province, adjacent to the building that inspired this study, to characterize the subsurface conditions. The SPT-N and corrected $N_{1,60}$ values obtained from the borehole log are presented in Figure 2. According to the borehole data, the groundwater table is located at a depth of 3 meters below the ground surface.

The soil profile consists of a 4-meter-thick sandy clay layer from the surface, underlain by an approximately 16-meter-thick gravelly sand layer. Based on the Standard Penetration Test (SPT) results from the ISK-275 borehole log, the average $N_{1,60}$ value of the upper sandy clay layer was calculated as 21. In contrast, the average $N_{1,60}$ value of the underlying gravelly sand layer was calculated as 6.

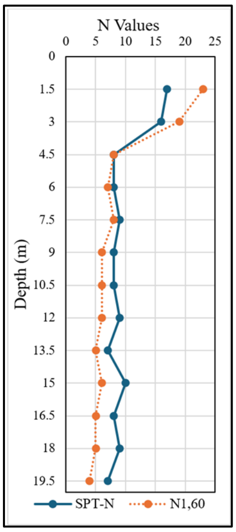

Figure 2. Variation of N values with depth based on borehole data

Based on the data obtained from the aforementioned borehole investigation, the soil model used in the numerical analyses was developed as shown in Figure 3. The uppermost 0.5 meters of the soil model represents a fill layer defined using the HS-Small soil model. Immediately beneath this layer, a 3.5-meter-thick silty clay layer with a plasticity index of 20% was defined. Below this, a 16-meter-thick sand layer with a relative density of 35% was included in the model. The underlying engineering bedrock layer described in the model has a thickness of 1 meter. The total width of the numerical model used in the analyses is 140 meters. At both lateral boundaries of the model, 2-meter-wide drained soil layers were incorporated to ensure compatibility with the overall model behavior. It should be noted that the adopted numerical modelling approach does not consider the influence of the position of the structure's center of gravity on the overall dynamic response. This simplification is acknowledged as a limitation of the study.

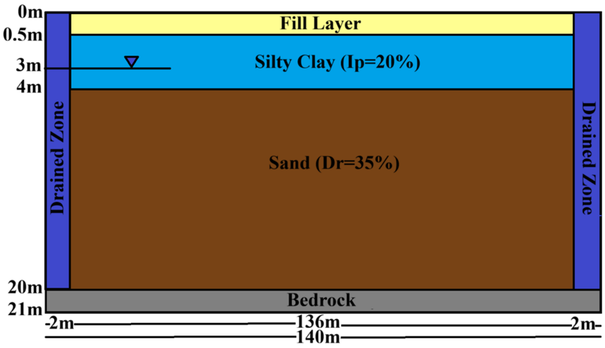

Figure 3. Soil profile used in the numerical analyses

2.2.1 *Material Parameters of the Soil*

Although the PM4Sand and PM4Silt constitutive models accurately simulate soil liquefaction behavior, they are not suitable for modeling initial stress conditions. Therefore, in the analyses conducted, the initial stress state was established using the Hardening Small Strain (HS-Small) soil model. The material parameters of the HS-Small model were calculated for a relative density of 35% and are presented in Table 2 (Brinkgreve et al., 2010). In the dynamic analyses performed using Plaxis 2D, the earthquake motion was not applied directly to the soil layer but instead transmitted through an underlying bedrock layer. The material parameters of the linear elastic engineering bedrock defined for this purpose are listed in Table 2.

Table 2. Material parameters of the HS-Small soil and linear elastic engineering bedrock models (Brinkgreve et al., 2010; Bastidas, 2016; PLAXIS Connect Edition, 2023).

Hardening Small Strain		Linear Elastic Engineering Bedrock	
Drainage Type	Drained	Drainage Type	Drained
γ_d (kN/m^3)	15.34	γ_d (kN/m^3)	22
γ_{sat} (kN/m^3)	19.36	γ_{sat} (kN/m^3)	22
e	0.695	e_{init}	0.5
Dr_0	0.35	Rayleigh α	0
E_{50ref} (MPa)	21	Rayleigh β	0
$E_{oed\ ref}$ (MPa)	21	E'_{ref} (MPa)	8
E_{urref} (MPa)	63	ν	0.2
m	0.59	G_{ref} (MPa)	3.33
c' (MPa)	0	E_{oed} (MPa)	8.889
Φ' (°)	33	V_s (m/s)	1219
$\gamma_{0.7}$	0.00017	V_p (m/s)	1991
G_{0ref} (MPa)	83.8		
ν	0.3		
P_{ref} (MPa)	0.1		
R_f	0.956		

For the selection of material parameters for the PM4Sand constitutive model—developed for simulating the dynamic behavior of sandy soils in geotechnical earthquake engineering applications—the recommended values from the PM4Sand manual were used based on the average relative density of 35% corresponding to the soil between depths of 4 m and 20 m in the reference borehole log. The primary input parameters were selected for Dr = 35%, $(N_1)_{60}$ = 6, and Vs_1 = 144 m/s. Default values were used for the secondary parameters, and the contraction rate parameter (h_{p0}) was calibrated using direct simple shear (DSS) tests.

For the PM4Silt constitutive model—developed to simulate the behavior of low-plasticity silty and clayey soils in earthquake engineering applications—the material parameters were selected based on the recommendations in the PM4Silt manual for a plasticity index (PI) of 20%, representative of the sandy clay soil between the ground surface and a depth of 4 m in the reference borehole log. The soil in this layer is classified as CL (low-plasticity clay) according to the USCS, is normally consolidated, has a plasticity index of 20%, a liquid limit (LL) of 42%, and a shear wave velocity (Vs) of 120 m/s. It consists of 70% kaolinite and 30% silica silt by dry mass (Price et al., 2015; Price et al., 2017). The PM4Sand and PM4Silt material parameters used in the analyses are provided in Table 3.

Table 3. Material parameters of the Pm4Sand and Pm4Silt constitutive models (Bastidas, 2016; Boulanger and Ziotopoulou, 2017, 2018)

Pm4Sand		Pm4Silt	
Drainage Type	Undrained A	Drainage Type	Undrained A
e	0.695	e_0	1
Dr_0	0.35	Su_{ratio}	0.35
G_o	476	G_o	345
h_{p0}	0.53	h_{p0}	1.2
e_{maks}	0.8	P_{atm} (kN/m^2)	101.3
e_{min}	0.5	n^G	1
Pa (MPa)	0.101	h_o	0.5
n_b	0.5	λ	0.18
n_d	0.1	Φ_{cv} (°)	25
Φ_{cv} (°)	33	$n^{b,wet}$	1
ν	0.3	$n^{b,dry}$	0.5
Q	10	n^d	0.3
R	1.5	A_{do}	0.8
		z_{max}	10
		c_z	20
		C_ϵ	0.25
		C_{GD}	3
		$C_{k\alpha f}$	4
		ν	0.3

2.2.2 *Material Parameters of the Structures*

In the analyses, a seven-story building model was defined by applying a "Line Load" on top of the foundation modeled as a "Plate" element, with each story load equal to 15 kPa. The material parameters of the shallow raft foundation, which has a diameter of 0.6 m and a width of 25 m, are presented in Table 4. Unreinforced piles are modeled as "Embedded Beam" elements in the analyses. The unreinforced piles, with an elastic modulus of 30 GPa, have a length of 6 meters, a diameter of 60 cm, and are spaced at 2-meter intervals. The material parameters of the piles are presented in Table 4. In this study, the pile-foundation connections were modeled as hinged. Therefore, the model does not account for moment transfer and cannot simulate tensile (uplift) axial forces in the piles. This simplification may slightly underestimate the vertical load transfer under seismic excitation and is considered a limitation of the study.

Table 4. Material parameters of shallow raft foundation and unreinforced piles (PLAXIS, 2023)

Shallow Raft Foundation		Unreinforced Pile	
Material Type	Elastic	Material Type	Elastic
w (kN/m/m)	20	γ (kN/m^3)	25
Rayleigh α	0.232	$L_{spacing}$ (m)	2
Rayleigh β	0.008	d (m)	0.6
EA (kN)	45E6	E (kN/m^2)	30E6
EI (kNm)	1.35E6	T_{max} (kN/m)	1E12
ν	0		
d (m)	0.6		

3 ANALYSIS RESULTS

In this section, the performance of buildings with different foundation systems during seismic soil liquefaction is examined based on the results of numerical analyses conducted in Plaxis 2D using the PM4Sand and PM4Silt constitutive models. The analyses were carried out using the earthquake record from the TK-3116 station located in the İskenderun district, corresponding to the first mainshock of the February 6, 2023 Kahramanmaraş Earthquakes.

To enable comparison of the performance of different foundation systems, all buildings were designed with the same number of stories, i.e., seven stories. The models include a building with a raft foundation system having one and two basement floors and buildings with unreinforced pile foundation systems designed as basement-free (foundation depth of 1 m), one basement floor (3 m foundation depth), and two basement floors (6 m foundation depth). All buildings were modeled using a soil profile developed from data from the ISK-275 borehole log. The variations in depth of settlement beneath the center of the building foundations, lateral displacements, shear strains, and excess pore-water pressure ratios due to seismic soil liquefaction were investigated. The settlement values calculated at the foundations were evaluated to assess the buildings' performance, considering maximum settlement, differential settlement, and angular rotation. These parameters were then compared against permissible limits defined in international standards and codes used in civil engineering practice.

Figure 4 presents the distribution of settlements obtained from the analysis conducted for the structure with unreinforced piles and two-storey basement floors. Lateral and bottom boundaries of the numerical model were positioned sufficiently far from the foundation to minimize artificial reflections and constraint effects. Minor strain localizations observed near the model edges are typical of finite model boundaries; however, sensitivity analyses confirmed that these boundary edge effects do not significantly influence the overall settlement pattern or the performance of the improved ground. The results of the analyses illustrating the variation of settlements and lateral displacements beneath the foundation centers of buildings with different foundation systems during liquefaction are presented in Figure 5.

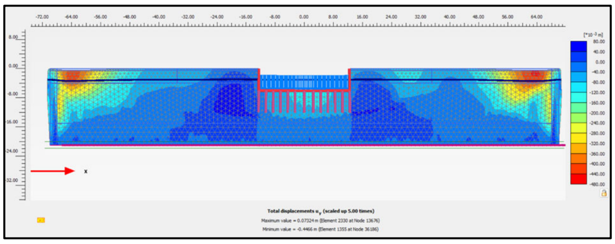

Figure 4. Distribution of settlements obtained from the analysis conducted for the structure with unreinforced piles and two-storey basement floors

When evaluating the variation in settlements with depth beneath the foundation centers of the structures, the largest settlements were observed under the soil beneath the building with an unreinforced pile foundation system without a basement floor. In contrast, the smallest settlements occurred under the soil beneath the building with an unreinforced pile foundation system featuring two basements. For both foundation systems, it was observed that settlements beneath the foundation decreased with increasing foundation depth. When evaluating lateral displacements with depth beneath the foundation centers of the structures, the largest lateral displacements were observed under the soil beneath the building with a shallow raft foundation and one basement floor. The smallest lateral displacements occurred under the soil beneath the building with a two-basement shallow foundation system.

The distribution of excess pore water pressure ratio for the analysis carried out with unreinforced piles and two-storey basement floors is presented in Figure 6. The variations in excess pore water pressure ratios and shear strains with depth occurring in the soil beneath the foundation centers of buildings with different foundations during liquefaction are presented in Figure 7.

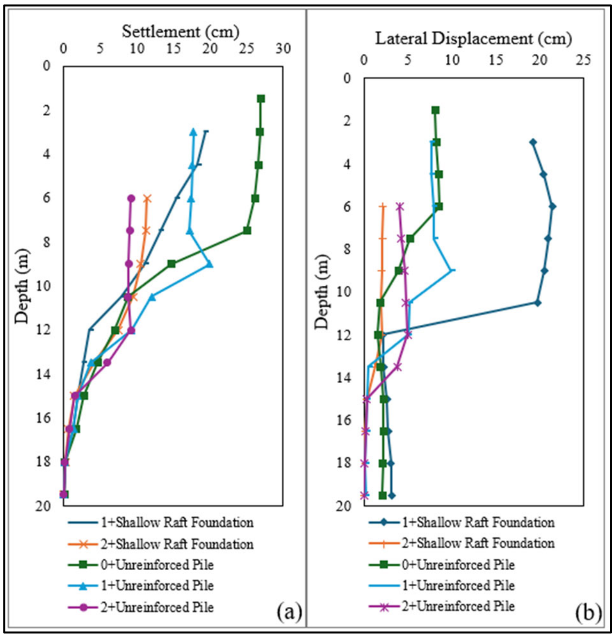

Figure 5. (a) Comparison of settlement variations with depth beneath the foundation centers of structures (b) Comparison of lateral displacement variations with depth beneath the foundation centers of structures

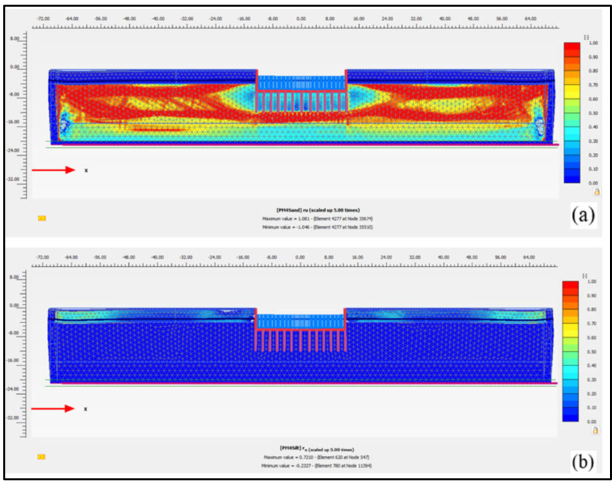

Figure 6. (a) Distribution of excess pore water pressure ratio in the Pm4Sand layer as a result of the analysis carried out with the structure with unreinforced piles and a two-storey basement floor (b) Distribution of excess pore water pressure ratio in the Pm4Silt layer as a result of the analysis carried out with the structure with unreinforced piles and a two-storey basement floor.

When examining the variation of excess pore water pressure ratio beneath the centers of the structures, it was observed that the excess pore water pressure ratio developed at different magnitudes at different soil depths beneath the buildings, making performance comparisons challenging. According to analyses using the PM4Sand model, liquefaction of the soil beneath almost all buildings was predicted.

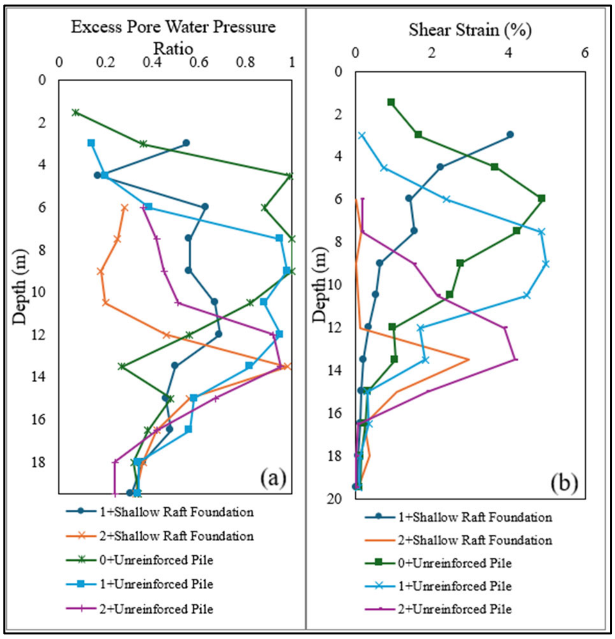

Figure 7. (a) Comparison of excess pore water pressure ratio variations with depth beneath the foundation centers of structures (b) Comparison of shear strain variations with depth beneath the foundation centers of structures

When evaluating the variation of shear strains with depth beneath the foundation centers of the buildings, the largest shear strains were observed in the soil beneath structures with unreinforced pile foundations without a basement and with one basement floor. The smallest shear strains were observed beneath the building with a two-storey basement floor and a shallow raft foundation system, and the building with a two-storey basement floor and an unreinforced pile foundation system. Furthermore, for both foundation systems, shear strains in the soil beneath the foundation decreased with increasing foundation depth.

The results of the numerical analyses of the maximum settlements, differential settlements, and angular rotation behavior of buildings with different foundation systems are presented in Table 5.

Table 5. Calculated total settlement, differential settlement, and angular distortion values at the foundations of the structures

Building Properties	Total Settlement	Differential Settlement	Angular Rotation
Structure with one basement floor and shallow raft foundation system.	53.8cm	34.51cm	0.748%
Structure with two basement floors and shallow raft foundation system.	11.41cm	7.09cm	0.036%
Structure without a basement floor and an unreinforced pile foundation system.	26.98cm	1.56cm	0.0228%
Structure with one basement floor and an unreinforced pile foundation system.	17.76cm	3.95cm	0.0356%
Structure with two basement floors and an unreinforced pile foundation	9.17cm	6.4cm	0.1148%

The evaluations showed that total settlement, differential settlement, and angular rotation behaviors of the buildings exhibited significant variations depending on the foundation system and the number of basement floors. For buildings with shallow raft foundations, the total settlement reached 53.8cm with one basement floor, whereas it decreased to 11.41cm with two basement floors. A similar trend was observed for differential settlement and angular rotation: the building with one basement exhibited a differential settlement of 34.51cm and an angular rotation of 0.748%, while these values were reduced to 7.09cm and 0.036%, respectively, for the building with two basement floors. For structures supported by unreinforced pile foundation systems, the building without a basement experienced the highest total settlement, reaching 26.98cm. Introducing basement levels significantly reduced settlements: the one-basement configuration resulted in 17.76cm, and the two-basement configuration further decreased total settlement to 9.17cm, with corresponding improvements in differential settlement and angular rotation values. Overall, these findings indicate that increasing the number of basement floors and employing unreinforced pile foundations both contribute positively to reducing settlement and rotational demands on the structures, enhancing their performance under seismic loading.

The total settlement values and angular rotation behaviors of buildings with different foundation systems during seismic soil liquefaction were evaluated according to the criteria established by the Canadian Foundation Engineering Manual (2006), as shown in Figure 8 (Canadian Geotechnical Society, 2006). When evaluating the total settlement values of the buildings according to the Canadian Foundation Engineering Manual (2006), it was observed that all buildings exceeded the allowable limits. Regarding angular rotation behavior, only the shallow foundation building with one basement floor exceeded the limit prescribed by the standard, while all other buildings remained within the permissible limits.

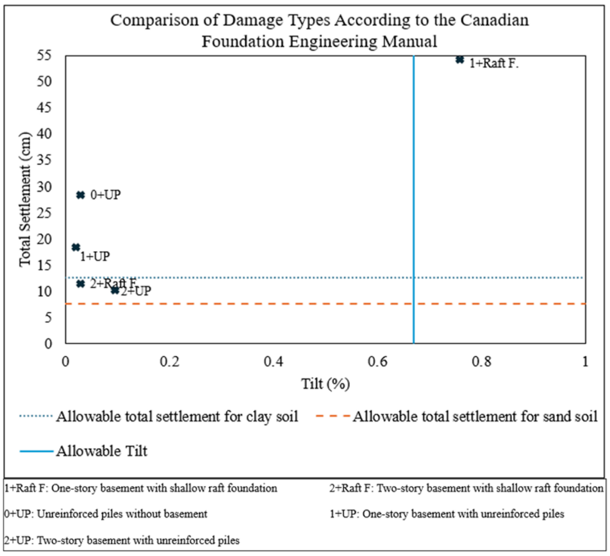

Figure 8. Comparison of Damage Types According to the Canadian Foundation Engineering Manual (2006)

4 CONCLUSIONS

Seismic waves generated by fractures in the earth's crust cause significant engineering problems in soils susceptible to liquefaction, where reductions in stiffness and shear strength may lead to structural damage or even collapse. Accordingly, the performance of structures designed with different foundation systems during liquefaction varies significantly. In this study, a layered soil profile inspired by the İskenderun district was used to evaluate the performance of structures with different foundation systems and foundation depths, using the

PM4Sand and PM4Silt constitutive models in Plaxis 2D. Structures with shallow raft foundation systems were modeled both without basements and with one basement; and structures on unreinforced pile foundations were modeled without basements, with one basement, and with two basements. As a result of the analyses, excess pore water pressure, shear strain, horizontal and vertical displacements with depth, total and differential settlements at the foundation floor, and angular rotation values of the buildings were calculated. These computed values were evaluated against international standards and regulations, and the performance of the structures was compared.

The findings indicate that increasing foundation depth improves structural performance by reducing settlements and deformations regardless of the foundation system. The best performance was observed in the structure with two basement floors and an unreinforced pile foundation. In contrast, the weakest performance was observed in the structure with a shallow raft foundation and a single basement.

Detailed numerical analyses of liquefaction-induced soil behavior and their effects on structural performance are crucial for selecting foundation type and depth.

5 ACKNOWLEDGEMENTS

The work described in this paper was supported by the Yıldız Technical University Scientific Research Projects Coordination Department, Project Number: FBA-2026-7567.

6 REFERENCES

Bastidas, A.M.P., 2016. Ottawa F-65 sand characterization. Ph.D. dissertation, University of California, Davis, USA.Bird, J.F., Bommer, A.R., Crowley, A.J. and Toma, A.P.G., 2005. A reliability-based approach to liquefaction-induced settlement of foundations. Soil Dynamics and Earthquake Engineering, 25(7–10), pp.651–662.

Boulanger, R.W. and Ziotopoulou, K., 2017. PM4Sand (version 3.1 Revised July 2018), A sand plasticity model for earthquake engineering applications. Scientific Report UCD/CGM-17/01. Davis, CA: University of California, Department of Civil and Environmental Engineering.

Boulanger, R.W. and Ziotopoulou, K., 2018. PM4Silt (Version 1), A silt plasticity model for earthquake engineering applications. Scientific Report UCD/CGM-18/01. Davis, CA: University of California, Department of Civil and Environmental Engineering.

Bray, J.D. and Dashti, S., 2014. Liquefaction-Induced Building Movements. Bulletin of Earthquake Engineering, 12(3), pp.1129–1156.

Brinkgreve, R.B.J., Engin, E. and Engin, H.K., 2010. Validation of empirical formulas to derive model parameters for sands. In: T. Benz and S. Nordal, eds. Numerical Methods in Geotechnical Engineering. Rotterdam: CRC Press, Balkema, pp.137–142.

Canadian Geotechnical Society, 2006. Canadian Foundation Engineering Manual. 4th ed. Richmond, BC: BiTech Publishers Ltd.

Casagrande, A., 1936. Characteristics of cohesionless soils affecting the stability of slopes and earth fills. Journal of the Boston Society of Civil Engineers, 23(1), pp.13–32.

Dafalias, Y.F. and Manzari, M.T., 2004. Simple plasticity sand model accounting for fabric change effects. Journal of Engineering Mechanics, 130(6), pp.622–634.

Mogami, T. and Kubo, K., 1953. The behavior of soil during vibration. In: Proceedings of the 3rd International Conference on Soil Mechanics and Foundation Engineering. Zurich, Switzerland, 1953. Vol. 1, pp.152–155.

PLAXIS, 2023. PLAXIS 2D 2023.2 Tutorial Manual 2D. Bentley Advancing Infrastructure.

PLAXIS, 2023. User defined soil models - PM4Sand: A sand plasticity model for earthquake engineering. PLAXIS Connect Edition V22.02. Bentley Advancing Infrastructure.

Price, A.B., Boulanger, R.W., DeJong, J.T., Parra Bastidas, A.M. and Moug, D., 2015. Cyclic strengths and simulated CPT penetration resistances in intermediate soils. In: 6th International Conference on Earthquake Geotechnical Engineering. Christchurch, New Zealand, 2015.

Price, A.B., DeJong, J.T. and Boulanger, R.W., 2017. Cyclic loading response of silt with multiple loading events. Journal of Geotechnical and Geoenvironmental Engineering, 143(10), p.04017080. https://doi.org/10.1061/(ASCE)GT.1943-5606.0001759.

Terzaghi, K. and Peck, R.B., 1948. Soil Mechanics in Engineering Practice. New York: Wiley.